RESEARCH ARTICLE OPEN ACCESS

Corrosion Inhibition of Carbon Steel In Sulfuric Acid by Sodium Caprylate

Saad Ghareba[1,*], Sasha Omanovic[2]
[1]Department of Chemical and Petroleum Engineering, Al-Mergib University, Alkhums Libya
*Corresponding author: smghareba@elmergib.edu.ly
[2]Department of Chemical Engineering, McGill University, Montreal, Quebec, Canada H3A 2B2

ABSTRACT
The interaction of a sodium salt of octanoic acid, sodium caprylate (SC), with a carbon steel (CS) surface was investigated, using range of experimental techniques. It was shown that SC acts as a good CS general corrosion inhibitor, yielding a maximum corrosion inhibition efficiency of 77%. This high inhibition efficiency is maintained even at higher temperatures. It was determined that SC inhibits both partial corrosion reactions, and can thus be considered to be a mixed-type inhibitor. The adsorption of SC on the CS surface was described by the Langmuir adsorption isotherm. It was found that this process is spontaneous, irreversible and driven by the entropy gain. The CS surface morphology was studied by SEM and it was demonstrated that SC is a very effective general corrosion inhibitor of CS. This also was confirmed by contact angle measurements which showed that the CS surface became more hydrophobic when the SC was added to the solution.
KEY WORDS: Corrosion inhibition, electrochemical impedance spectroscopy, Tafel slopes, adsorption, scanning electron microscopy, contact-angel, Carbon steel.

I. INTRODUCTION

Corrosion of steel represents one of the major problems that occur in oil and gas industry. Although carbon steel is widely employed as a construction material for pipe work in the oil and gas production, its corrosion resistance is very low. Therefore, the most common method, in order to increase its resistance and thus to minimize corrosion, is by using corrosion inhibitors which have been widely used and considered as a first line of defense against corrosion. The corrosion protection by these inhibitors is based mostly on the modification of metal surfaces by the adsorption of these molecules and the subsequent formation of a protective (blocking) layer that minimizes access of the corrosive electrolyte to the surface. However, many common corrosion inhibitors used in the oil, and also other industries are not environmentally friendly [1, 2]. Therefore, there is increased attention directed towards the development of environmentally compatible, nonpolluting corrosion inhibitors. Naturally occurring biological molecules are of considerable interest as possible corrosion inhibitors [3-11]. Most of the well-known inhibitors are organic compounds containing hetero atoms such as nitrogen, sulfur, phosphorus and/or oxygen atoms [12, 13]. Recently, self-assembled-monolayers (SAMs) have attracted a great deal of attention as corrosion inhibitors for various applications [14-19]. The advantage of the molecular self-assembly process lays mostly in the wide variety of functional groups of self-assembling molecules. Self-assembly is a spontaneous process taking place by immersion of an appropriate substrate into a solution of surfactant molecules, consisting of adsorption and self-organized formation of highly ordered molecular monolayers resulting in a dense and stable structure. Usually alkane derivatives with one or two functional groups are used to build up self-assembled mono- or multilayers. The head group of the molecule is responsible for the strong metal/molecule interaction that is usually chemisorption. The other functional group determines the physical and chemical properties of the modified surface. This functional group is usually selected for the requirements of application or further treatments of modified metals. The ability to tailor both head and tail groups of selfassembling molecules provides desired control of the structure and chemical properties of surface at the molecular level and thus should be considered as a potential technique for the construction of future organic materials.

The aim of this work research was to investigate the possibility of SC as a steel corrosion inhibitor in acidic media, H_2SO_4, and to determine the mechanism of its corrosion inhibition.

II. EXPERIMENTAL PROCEDURES

2.1. Chemicals and solutions

The corrosion inhibitor, sodium salt of octanoic acid; sodium caprylate, SC, 99 % pure, was purchased from Sigma-Aldrich Canada, Ltd, (product no. 71339) and was used as received without further purification. The chemical structure is shown in

Figure 1. Corrosion test solutions (electrolytes) of sulfuric acid were prepared by diluting concentrated sulfuric acid (98%) to the required concentration using deionized water. The SC stock solution was prepared by dissolving the required amount of SC powder in corresponding corrosion test-electrolyte. Deionized water (resistivity = 18 MΩ cm) was used in the preparation of all aqueous solutions.

2.2. Electrochemical equipment

A standard three-electrode, one compartment cell was used for electrochemical (i.e. corrosion) measurements. The counter electrode was a platinum electrode (mesh) of high purity (99.99%), sealed in soft glass, and stored in 98% H_2SO_4 when not in use. The reference electrode was saturated calomel electrode (SCE). All potentials in this work are referred to SCE. The working electrode was prepared from a CS rod (see Table 1 for the chemical composition of the steel) sealed with epoxy resin to give a two-dimensional surface exposed to the electrolyte. The geometrical area of the CS electrode was 0.54 cm^2, but all the surface-area-dependent values used in this paper (current, impedance, resistance, and capacitance) are normalized with respect to the geometric surface area of the electrode.

Electrochemical techniques were done using an AUTOLAB potentiostat/galvanostat PGSTAT 30 handled by FRA2 and GPES v. 4.9 software. The chemical identification of the adsorbed SC layer was done using a Bruker FTIR spectrometer, Tensor 27/PM50, equipped with an external polarization-modulation module and liquid nitrogen cooled MCT detector. To study the surface morphology, scanning electron microscopy (FEG-SEM Phillips XL30) technique was employed.

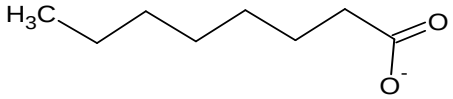

Figure 1 Chemical structure of sodium caprylate molecule

Table 1 Chemical composition of carbon steel.

Element	Content (wt.%)
Fe	Balance
C	0.130
Cu	0.162
Cr	0.030
Co	0.016
Mn	0.790
Mo	0.053
Nb	0.004
Ni	0.100
P	0.005
S	0.013
Si	0.188
Sn	0.028
Ti	0.001
V	0.007

2.3. Experimental Methodology

Prior to each experiment, the working electrode was wet polished with 600, 1500, and finally 1200/4000 grit sand paper, thoroughly rinsed with deionized water, to give a mirror-like surface. After polishing, the electrode was degreased with ethanol in an ultrasonic bath (~5 min) and then rinsed with deionized water. The electrode was then immersed in the electrolyte and equilibrated for 1 hr at open-circuit potential (OCP), followed by a specific type of experiment.

All measurements were carried out in oxygen-free solutions, which were achieved by continuous purging of the solution with argon gas (pre-purified grade purity) for at least 30 minutes prior the experiment and kept bubbling through the solution during the measurement. This bubbling also provided a well-mixed bulk solution.

III. RESULTUS AND DISCUSSION

3.1. Effect of SC concentration using Electrochemical Impedance Spectroscopy (EIS)

EIS technique was applied to investigate the electrode/electrolyte interface and processes that occur on the CS surface at open circuit potential (OCP) in the presence and absence of SC in the solution. To ensure complete characterization of the interface and the surface processes, EIS measurements were made over seven frequency decades, from 100 kHz to 10 mHz with the alternating current (AC) root-mean-square voltage amplitude of ±10 mV. Figure 2 shows an example of EIS spectra recorded on the CS electrode in SC-free solution (0 mM SC) and in the 0.5 M H_2SO_4 solutions containing various concentration of SC. The measurements were made after the stabilization of the electrode at OCP for one hour, and at room temperature. Nyquist plot shows the presence of only one time constant.

In order to both qualitatively and quantitatively describe the impedance behavior of the system, and thus to obtain a physical picture of the electrode/electrolyte interface and the processes occurring at the CS surface, the experimental data were fitted by using the nonlinear least-square fit analysis (NLLS) software and electrical equivalent circuits (EEC) presented in Figure 3 [20]. Figure 3 shows the EEC that describes a response of a one-time constant process, and has the following meaning: R_{el} (Ω) is the Ohmic resistance between the working and reference electrodes; R is the charge transfer resistance related to the corrosion reaction occurring at the OCP; CPE (F s^{n-1}) is the capacitance of the double-layer at the electrode/electrolyte interface, and is represented in terms of the constant-

phase-element, *CPE*. The impedance of a constant-phase element is defined as [20-23] $Z_{CPE} = (CPE(j\omega)^n)^{-1}$, with $-1 \le n \le 1$, where the constant *CPE* is a combination of properties related to both the surface and electroactive species and is independent of frequency. When the *CPE* power n is close to unity, the *CPE* can be considered to be equivalent to capacitance. On the other hand, when $n = 0$, the *CPE* becomes equivalent to resistance ($n = 0 \rightarrow F\, s^{n-1} = \Omega$). Deviation of n from unity, i.e. from the behavior of a pure capacitor, indicates the presence of inhomogeneities at the microscopic level of the electrode/electrolyte interface (surface roughness, adsorbed species, *etc.*) [24, 25]. The EEC in Figure 3 was used to model the response of the system characterized by only one time constant (the response in the absence of SC in the electrolyte, and also in the presence of SC. A very good agreement between the experiment (symbols) and the model (lines) was obtained at each SC concentration.

The spectra in Figure 2 show that the diameter of the semicircle increases with the increase in SC concentration in the electrolyte. The modeling procedure gave the charge-transfer resistance values that are listed in Table 2.

Table 2 Dependence of the charge transfer resistance on the concentration of SC in the electrolyte. The data were obtained by modeling the EIS spectra recorded in 0.5 M H_2SO_4 at pH 0.25 and at temperature 295 K.

c (mM)	0	3.5	5	6	7	8	9	10	12	15	20	30
R (Ω cm^2)	49	100	103	110	114	133	155	162	179	196	199	214

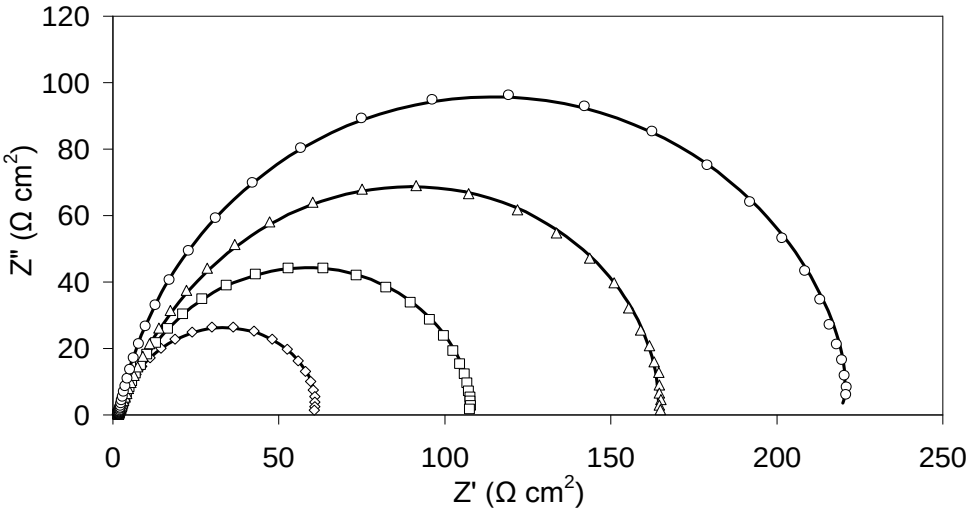

Figure 2 EIS as a Nyquist plot of CS recorded at different SC concentrations in 0.5 M H_2SO_4 at 295 K. (◊) 0 mM SC, (□) 5 mM SC, (Δ) 10 mM SC, and (○) 30 mM SC. Symbols are experimental data and solid lines represent the simulated spectra.

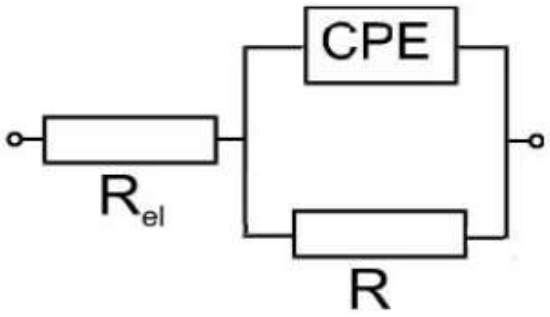

Figure 3 EEC model used to fit EIS data recorded on the carbon steel electrode.

Now, from the charge-transfer values in Table 2, the corresponding inhibition efficiency (η_i) was calculated by using:

$$\eta_i = \left(1 - \frac{R_0}{R_i}\right) \times 100 \quad (1)$$

and are graphically presented in Figure 4. From this figure, it can be seen that the inhibition efficiency gradually increases with an increase in SC concentration in the solution, and reaches a plateau at ca. 70% at the threshold SC concentration of ca. 17 mM SC. This indicates that, under the experimental conditions applied, in order to reach maximum inhibition efficiency, the minimum inhibitor concentration should not be below 17 mM.

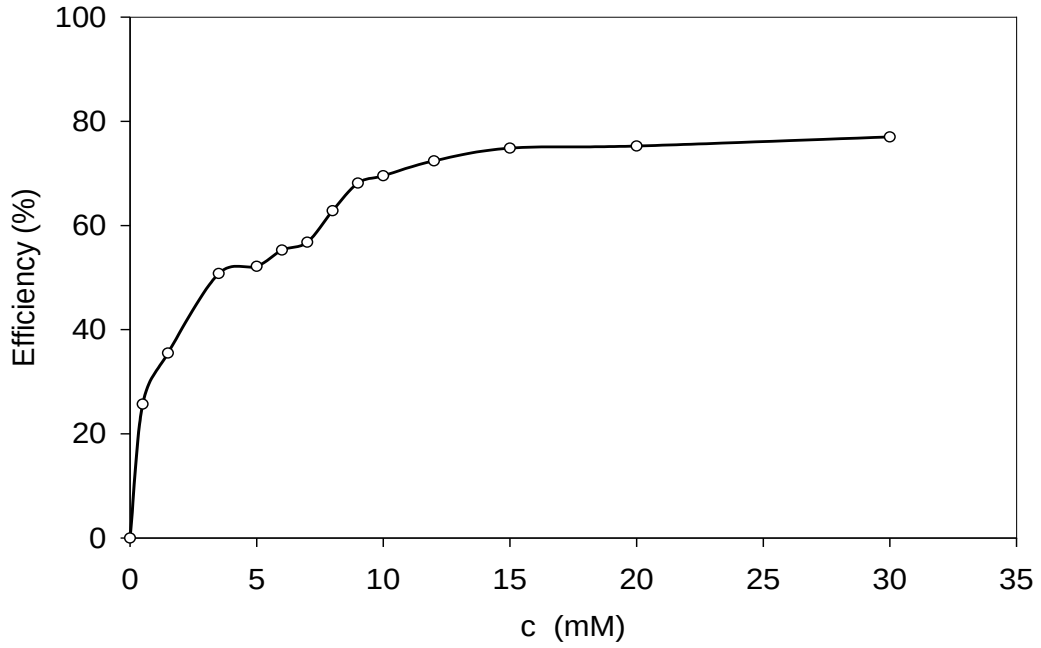

Figure 4 Corrosion inhibition efficiency of CS derived from EIS measurements done at various concentrations of SC in 0.5 M H_2SO_4. The data was obtained at 295 K.

3.2. Adsorption isotherm

The graph in Figure 4 shows a typical adsorption-isotherm shape. More specifically, it displays a behaviour that characterizes the formation of a saturated adsorption monolayer. Assuming that the inhibition efficiency, η, is proportional to the surface coverage by SC, θ [26-28], it is possible to treat the data in Figure 4, at least in the first approximation, using an adsorption isotherm. Several isotherms have been tested, but the best agreement was obtained when the Langmuir isotherm [27, 29]:

$$\frac{c}{\theta} = \frac{1}{B_{ads}} + c \quad (2)$$

where c (mol cm^{-3}) is the equilibrium concentration of the adsorbate in the bulk solution, θ is the surface coverage at particular adsorbate concentration, B_{ads} (cm^3 mol^{-1}) reflects the affinity of the adsorbate molecules toward adsorption sites. It is clearly seen from Figure 5 that the agreement between the experimental data (symbols) and the model (line) is very good (R^2= 0.994). The parameter B_{ads} could be defined and valuated at a constant temperature from the following [29, 30]:

$$B_{ads} = \frac{1}{c_{solvent}} \exp\left(\frac{-\Delta G_{ads}}{RT}\right) \quad (3)$$

where R (J $mol^{-1}K^{-1}$) is the gas constant, T (K) the temperature, ΔG_{ads} (J mol^{-1}) is the Gibbs energy of adsorption and $c_{solvent}$ is the molar concentration of solvent which is, in case of water, equal to 55.5 mol dm^{-3}. This parameter can be correlated with the Gibbs energy of adsorption, according to Eq.(3). The intercept of the line in Figure 5 yielded B_{ads}=354.61 dm^3 mol^{-1}, and using Eq.(3), the Gibbs energy of adsorption of SC on the CS surface at 295 K was calculated to be -24.09 kJ mol^{-1}. The negative value of Gibbs energy of adsorption indicates that the SC adsorption process is spontaneous.

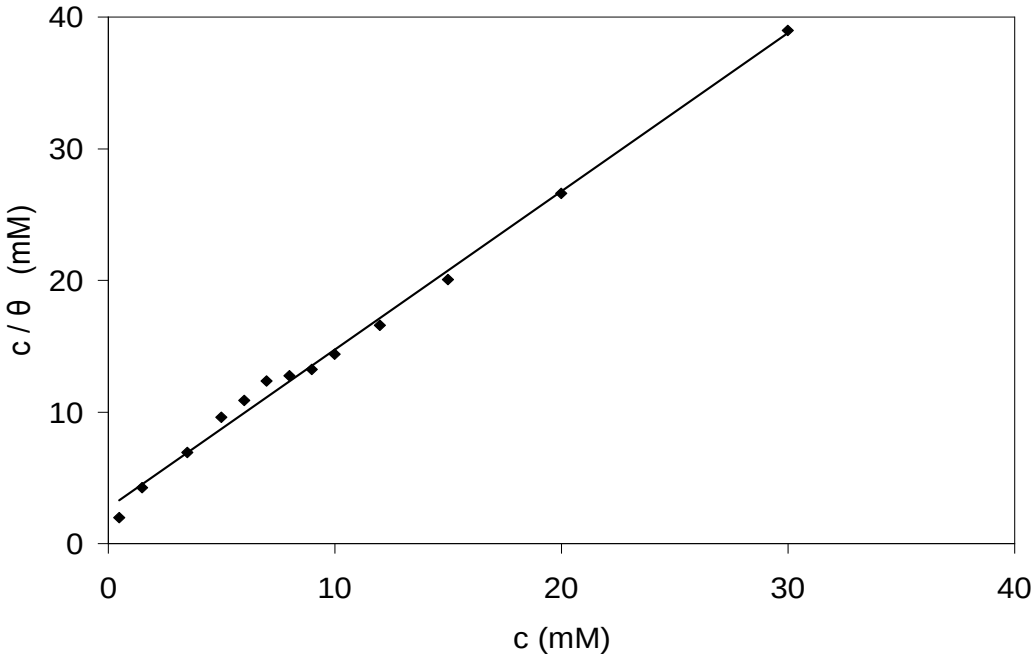

Figure 5 Linearized form of the Langmuir adsorption isotherm for adsorption of SC onto the CS surface. The data was obtained from Figure 4.

3.3. Effect of temperature

The effect of temperature on the inhibition effect of SC on carbon steel corrosion was studied over a wide temperature range, from 295 K to 323 K. In this study, EIS measurements were carried out by using two different SC concentrations 0 mM and 30 mM. Figure 6a shows a set of EIS spectra recorded at different temperatures in the absence of SC in the solution. With an increase in temperature, the diameter of the semicircle decreases, i.e. the charge-transfer resistance decreases, which is due to the increased corrosion rate. This is a typical behavior, since with an increase in temperature, the corrosion reaction kinetics also increases, and thus the corrosion rate. Quite the same behaviour was observed in the presence of 30 mM of SC in the solution (Figure 6b). However, by comparing the charge-transfer values at a fixed temperature, it is obvious that SC acts as a good corrosion inhibitor in the whole temperature range.

The results in Figure 6 show that the rate of corrosion increases with increasing temperature. Table 3 lists charge-transfer (i.e. corrosion) resistance values calculated in the absence and presence of SC in the electrolyte. The corresponding corrosion inhibition efficiency is also given. It is obvious that the corrosion efficiency of the inhibitor remains almost constant in the whole temperature range ($79 \pm 4\%$), which indicates that the SC molecule is chemically stable in the investigated temperature range, and that the mechanism of its corrosion inhibition does not change. Hence, SC seems to be a good inhibitor candidate even at higher temperatures.

Table 3 Dependence of the charge transfer resistance on temperature obtained from EIS measurements recorded on CS in the absence and presence of SC in 0.5 M H_2SO_4. The table also shows the corresponding corrosion inhibition efficiency.

T (K)	R (Ω cm^2)		Efficiency (%)
	0 mM SC	30 mM SC	
295	49.3	214.4	77
303	32.9	171.2	81
308	24.0	90.6	74
313	11.5	53.4	79
323	2.8	18.0	85

The EIS data was treated in the same way as in Figures 4 and 5, and the corresponding Gibbs energy of adsorption, $\Delta G_{ads,}$ was calculated, and presented in Figure 7. Subsequently, using that:

$$\Delta G_{ads} = \Delta H_{ads} - T\Delta S_{ads} \quad (4)$$

the enthalpy and entropy of adsorption was calculated to be ΔH_{ads} = 62 kJ mol^{-1}, and ΔS_{ads} = 0.28 kJ mol^{-1}K^{-1}, respectively. The enthalpy value demonstrates that the adsorption of SC on the CS surface is endothermic. Nevertheless, the relatively high negative Gibbs energy values (Figure 7) demonstrate that the overall adsorption process is highly spontaneous. Therefore, the major contribution to this spontaneity has to come from a *positive* gain in entropy. Indeed, the average value of the $T\Delta S_{ads}$ product is 86±3 kJ mol^{-1}. Therefore, the large positive gain in entropy seems to be the main contributor to the driving force for the adsorption of SC on CS. Our opinion is that the major contribution to the entropy gain in the system comes from the loss of the order of water molecules adsorbed on the CS surface upon SC adsorption. Under the influence of the electric charge on the CS surface, the adsorbed water molecules are highly ordered on the electrode surface [31], but when displaced by SC molecules, this high degree of order significantly decreases due to the random orientation of the displaced molecules in the bulk solution. This results in an overall increase in the positional degree of freedom of the system, *i.e.* an entropy gain. On the other hand, adsorbed SC molecules lose positional degrees of freedom, but this effect is largely overcome by the positive entropy contribution coming from water. Some other entropycally governed processes investigated in our laboratory include the adsorption of caffeine on a positively charged platinum surface [32], and also the adsorption of several proteins, such as yeast alcohol dehydrogenase, on a Pt surface [33], *β*-lactoglobulin on stainless steel [34], and bovine serum albumin on Ti [35].

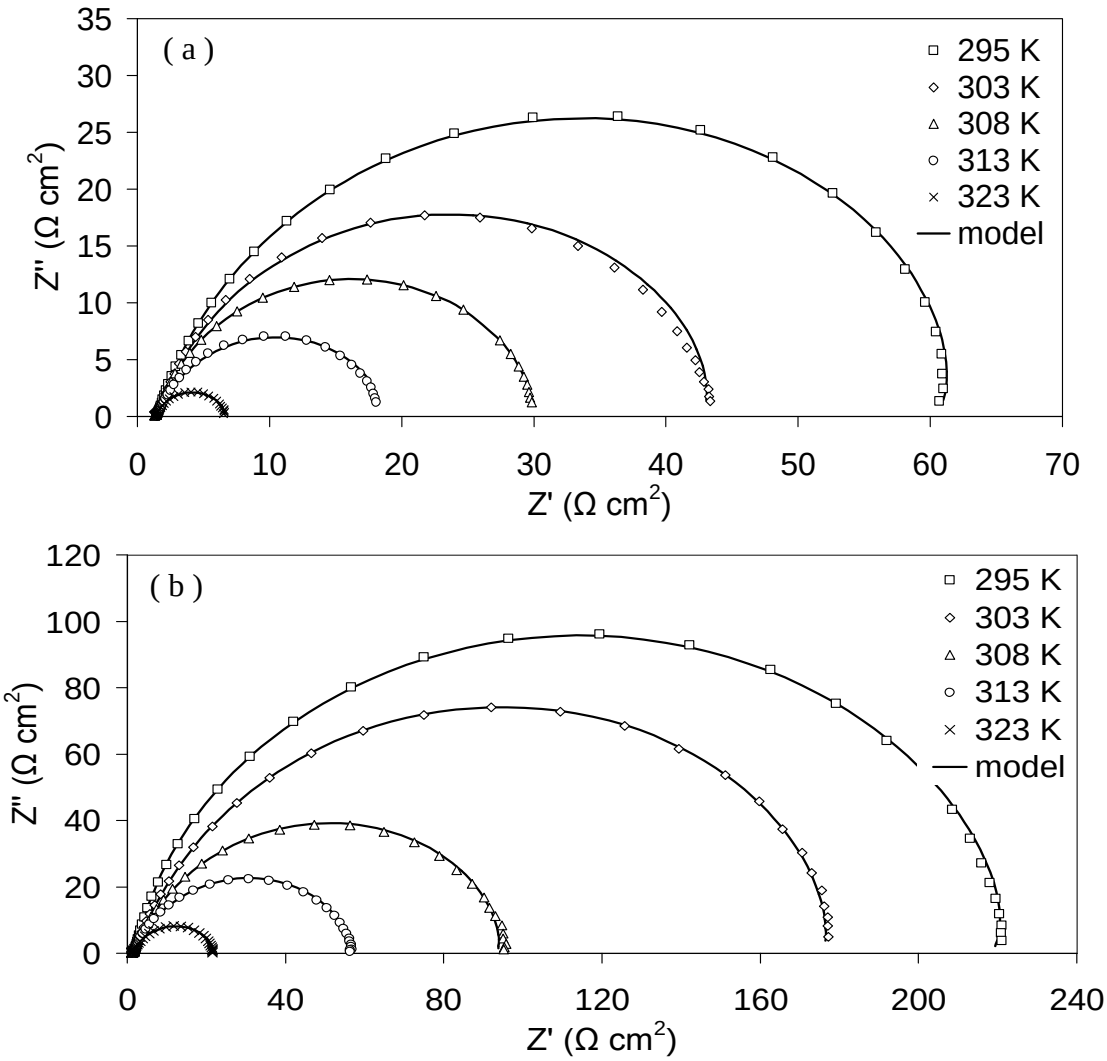

Figure 6 Nyquist impedance plots for carbon steel recorded at different temperatures in 0.5 mM H_2SO_4 (a) in the absence, and (b) presence of 30 mM of SC.

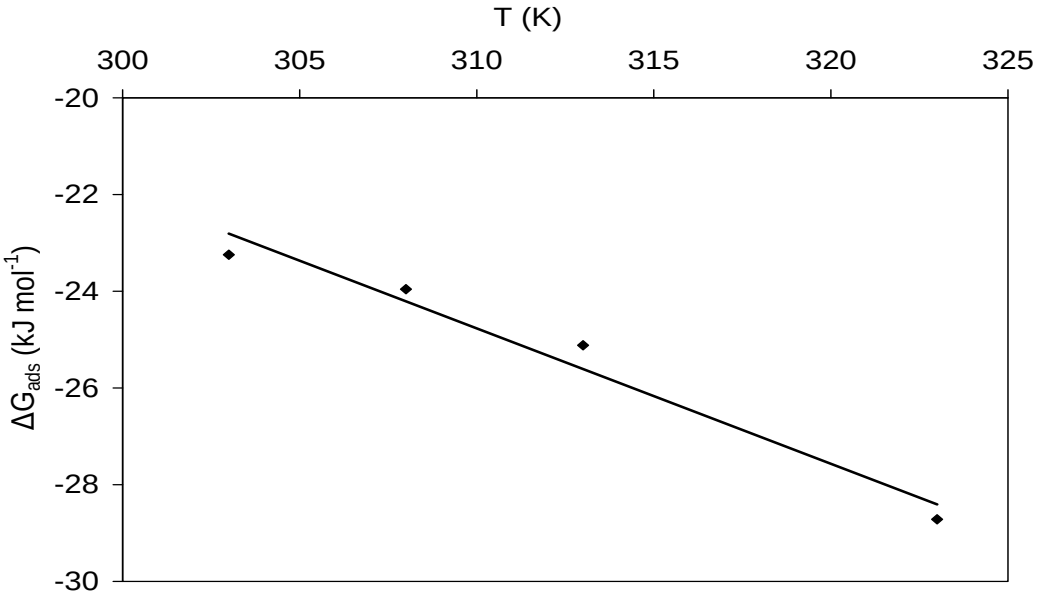

Figure 7 The dependence of Gibbs energy of adsorption on temperature. The data were obtained from EIS measurements recorded on CS at OCP and over a wide range of SC concentration in the bulk electrolyte.

3.4. Linear Tafel DC polarization

EIS is a technique of choice to study corrosion behaviour of various materials. However, it does not provide the information on the kinetics of partial corrosion reactions. For this purpose, linear Tafel DC polarization technique is used. In this work, the technique was used to study the behaviour of CS in the presence and absence of SC in in 0.5 M H_2SO_4 solution. Basically, after each EIS measurement, the Tafel measurement was made by polarizing the electrode ±0.2 V around OCP at a slow scan rate (1 mV s^{-1}). Figure 8 shows that with an increase in the concentration of SC in the bulk solution, both the cathodic and anodic current decreases.

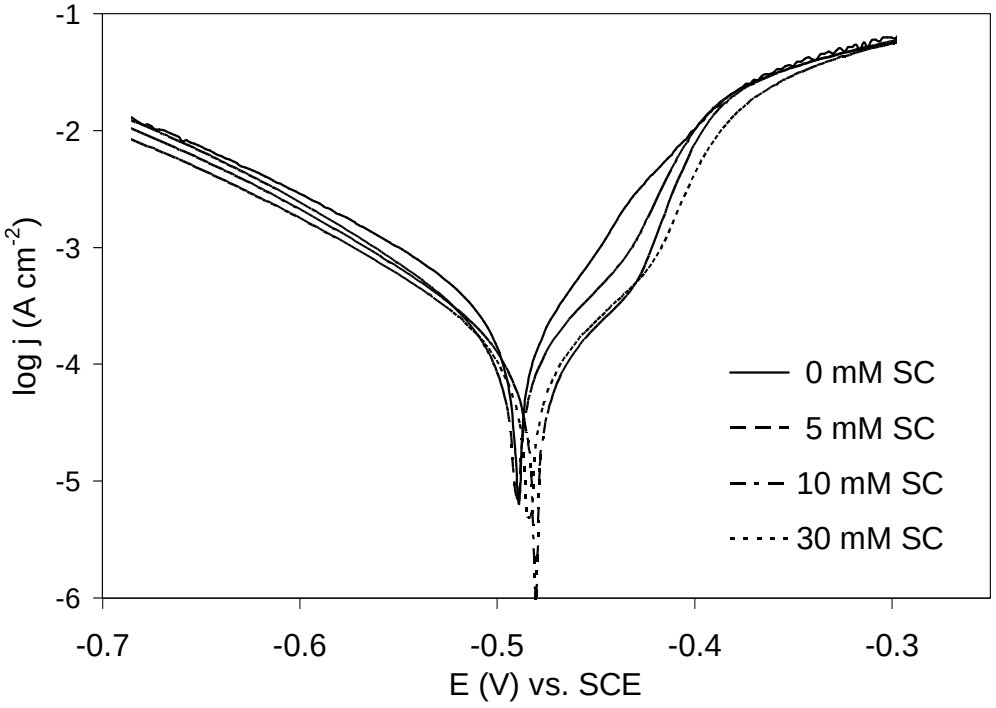

Figure 8 Tafel plots of the CS electrode recorded at 295 K in 0.5 M H_2SO_4 containing various concentrations of SC. Scan rate was 1 mV s^{-1}.

The cathodic behaviour of the CS in the absence of CS in the solution is characterized by the reduction of hydrogen:

$$2H^+ + 2e^- \rightarrow H_2 \quad (5)$$

On the other hand, the anodic reaction, which is dissolution of iron, is a complex reaction, and its detailed mechanism is not a topic of current investigation. A simplified anodic iron corrosion mechanism could be presented as:

$$Fe + 2OH^- \rightarrow Fe(OH)_2 + 2e^- \quad (6)$$

The results in Figure 8 show that when SC is increased in the corrosive electrolyte, the partial cathodic and anodic currents decrease. Therefore, since the SC inhibits both partial reactions, it can be considered as a *mixed type* inhibitor.

In order to quantify the extent of corrosion inhibition by SC, it is necessary to determine the corrosion current (which is directly proportional to the corrosion rate) in the presence and absence of SC. This is done by extrapolating the linear part of the anodic and cathodic Tafel slopes to corrosion potential ($E_{corr.}$ or OCP) [36], and the intersection of the slopes gives the corrosion current, $j_{corr.}$. The corresponding values are presented in Table 4. It is evident that the corrosion current in the presence of SC in the solution is considerably lower, which shows the inhibitive effect of SC. To quantify this effect, the corrosion inhibition efficiency (η_i) was also calculated using the following equation [21, 22, 26]:

$$\eta_i = \left(1 - \frac{j_{corr,i}}{j_{corr,0}}\right) \times 100\% \quad (7)$$

where $j_{corr.,i}$ (A cm^{-2}) is the corrosion current at a particular SC concentration, *i*, and $j_{corr.,0}$ is the corrosion current in the absence of SC in the solution. Using this equation, the corresponding inhibition efficiency (η_i) was also calculated and presented in Figure 9. The obtained trend is very similar to the trend observed in EIS measurements (Table 2 and Figure 4). Thus, although the two used techniques are completely different (DC vs. AC), the obtained results agree, thus independently validating the corrosion efficiency values and trends obtained.

Table 4 Corrosion current density ($j_{corr.}$) calculated form Tafel measurements recorded on CS in 0.5 M H_2SO_4 containing various concentrations of SC. T = 295 K.

c (mM)	0	1	3.5	5	6	9	10	12	15	20	30
$j_{corr.}$ (μA cm^{-1})	216	211	136	125	121	109	95	87	81	82	64

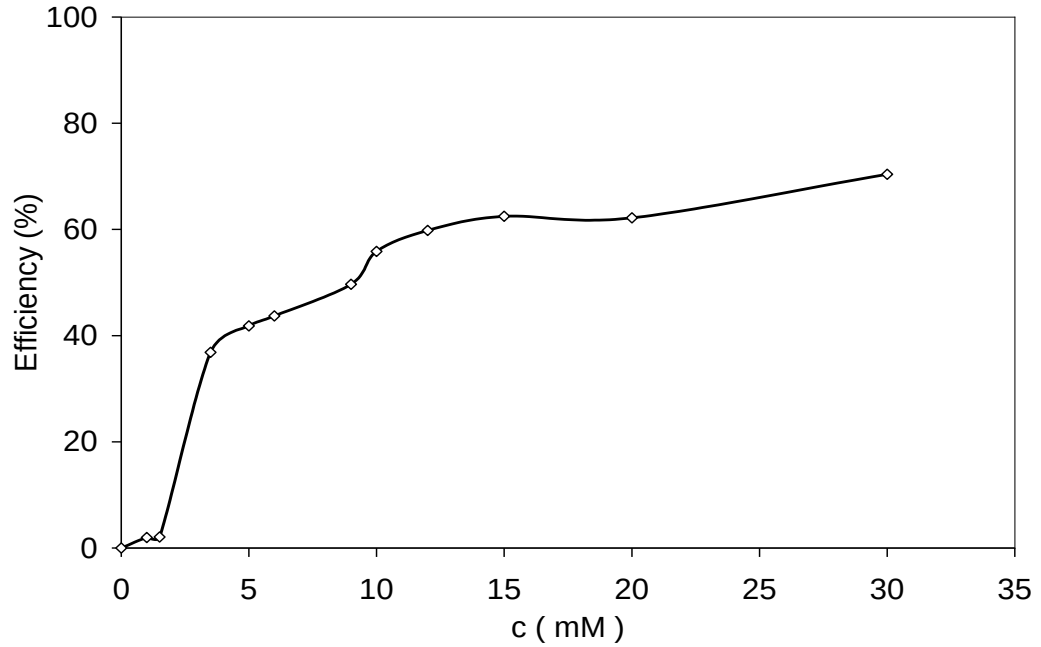

Figure 9 Corrosion inhibition efficiency of CS derived from Tafel measurements done at various concentrations of SC in 0.5 M H_2SO_4. The data was obtained at 295 K.

3.5. Scanning electron microscopy

Scanning electron microscopy (SEM) was used to obtain the information on the morphology of the CS surface corroded in the presence and absence of the inhibitor. The technique has already been used to observe the morphology of a corroded surface in the presence and absence of inhibitors [23]. Figure 10a demonstrates that in the absence of the inhibitor in

the solution, the corrosion of the surface is extensive. On the other hand, the image of the CS surface corroded in the presence of 30 mM of SC in the solution, Figure 10b shows a clean, not corroded surface. The small cracks seen on the surface were present even before the immersion of the surface in the corrosive electrolyte, and are a consequence of the polishing of the surface with alumina paper. Hence, these images also demonstrate that SC is a very effective general corrosion inhibitor of CS at low pH values.

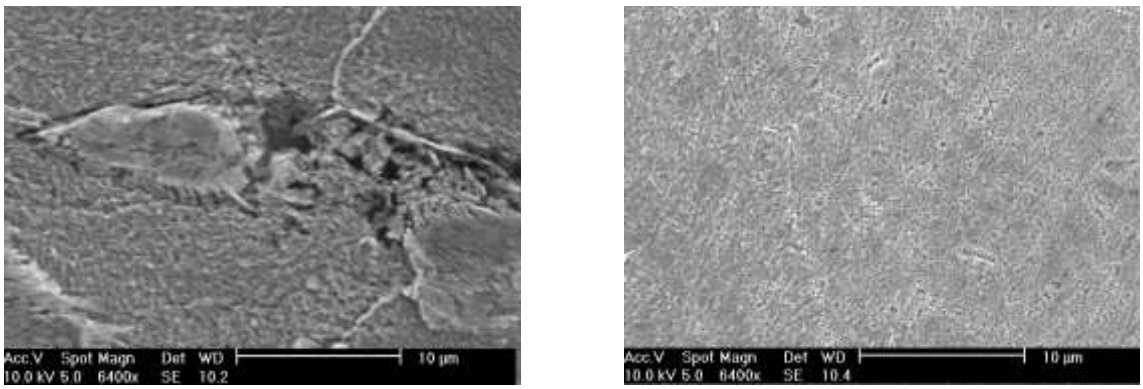

(a) (b)

Figure 10 SEM micrographs of a carbon steel surface taken after 17 hours of immersion of the surface in (a) pure 0.5 M H_2SO_4, and (b) in 0.5 M H_2SO_4 containing 30 mM of SC.

3.6. Contact-angle measurements

SC is an amphipilic molecule, consisting of the hydrophilic carboxylate head, and the hydrophobic alkyl chain. Hence, the CS surface covered by SC (Figure 10b) should yield a higher degree of hydrophobicity than the surface that corroded in the solution containing no SC (Figure 10a). In order to investigate this, contact angle measurements were done on two surfaces corroded for 24 hours in 0.5 M H_2SO_4 in the absence and presence of 30 mM of SC. Figure 11a shows the deionized water droplet on the surface corroded in the absence of the inhibitor in the solution. The corresponding contact angle was determined to be ca. 48º. This value shows that the corroded CS surface is hydrophilic. On the other hand, Figure 11b shows the contact angle measurement on the CS surface corroded in the presence of SC in the solution. The contact angle value in this case was determined to be ca. 103º, which indicates that the CS surface is becoming more hydrophobic. W. Furbeth *et al.* [37] measured a contact angle of 18.5º on passivated iron immersed in aqueous phosphonic acid solutions. This low value indicates high hydrophillicity of the surface. On the other hand, when the surface was modified by a dodecyl-phophonic and bithiophenic-hexane-phosphonic acid SAM, a contact angle of ca.148.5º and ca.121.7º was measured, respectively, demonstrating that the formed SAMs significantly increased the hydrophobicity of the surface.

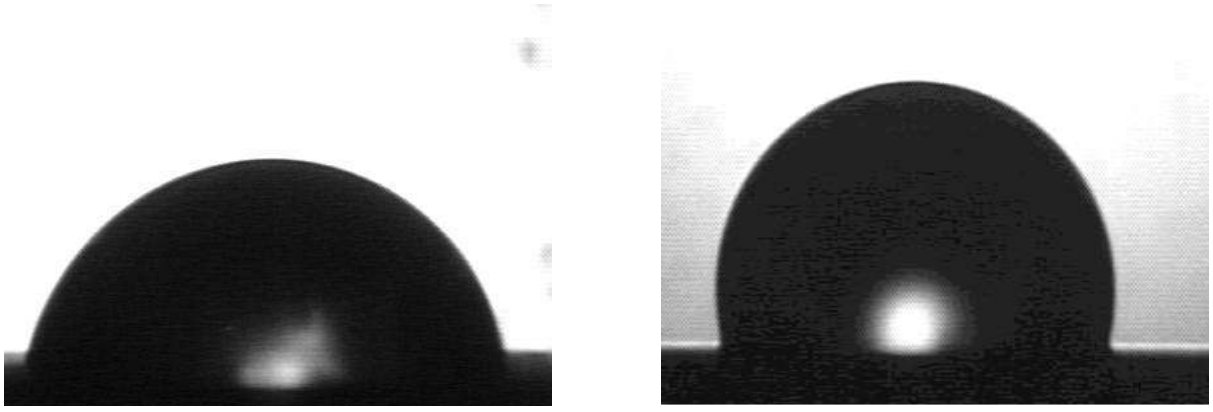

(a) **(b)**

Figure 11 Contact angle measurements on the CS surface that was kept for 24 hours in a 0.5 M H_2SO_4 solution (a) without SC, and (b) containing 30 mM of SC.

IV. CONCLOSION

The possibility of using a sodium salt of octanoic acid, sodium caprylate (SC), as a corrosion inhibitor was investigated, using Tafel polarization, EIS, contact-angle and SEM techniques.

- EIS and Tafel polarization measurements were used to evaluate the corrosion inhibition efficiency of SC. A very good agreement between results obtained by the two techniques was demonstrated.
- An equivalent-electrical-circuit approach was used to describe the structure of the steel/SC/electrolyte interface, to model EIS data.
- Tafel measurements revealed that SC inhibits both partial corrosion reactions, and can thus be considered to be a mixed-type inhibitor.
- Temperature-dependant measurements revaluated that SC maintains its high corrosion inhibition efficiency up to 323K, which indicates that the adsorbed SC layer is chemically stable in the investigated temperature range.
- The adsorption of SC at pH 0.25 was described by the Langmuir adsorption isotherm. The corresponding thermodynamic values showed that the SC adsorption is a highly spontaneous process, driven by the entropy gain, which is due to the displacement of water from the CS surface.

V. ACKNOWLEDGMENTS

The authors express their sincere acknowledgment to the Ministry of Higher Education and Al-Mergib University, Alkhums Libya, McGill University and the Natural Science and Engineering Research Council of Canada for providing the support for this research.

REFERENCES

[1.] G. Wranglen, Introduction to Corrosion and Protection of Metals. 1985, New York City, New York Chapman and Hall. 172.
[2.] H.H. Uhlig and R.W. Fevie, Corrosion and Corrosion Control. 1985, New York City, New York John Wiley and Sons. 263.
[3.] A. Bouyanzer, B. Hammouti, and L. Majidi, Pennyroyal oil from Mentha pulegium as corrosion inhibitor for steel in 1M HCl. Materials Letters, 2006. 60: p. 2840.
[4.] F. Deflorian and I. Felhosi, Electrochemical Impedance Study of Environmentally Friendly Pigments in Organic Coatings. Corrosion, 2003. 59: p. 112.
[5.] G. Blustein, et al., Study of iron benzoate as a novel steel corrosion inhibitor pigment for protective paint films. Corrosion Science, 2007. 49: p. 4202.
[6.] M. Salasi, et al., The electrochemical behaviour of environment-friendly inhibitors of silicate and phosphonate in corrosion control of carbon steel in soft water media. Materials Chemistry and Physics 2007. 104: p. 183.
[7.] M.A. Migahed, et al., Effectiveness of some non ionic surfactants as corrosion inhibitors for carbon steel pipelines in oil fields. Electrochimica Acta 2005. 50: p. 4683.
[8.] M.A. Quraishi and D. Jamal, Technical Note: CAHMT—A New and Eco-Friendly Acidizing Corrosion Inhibitor. Corrosion, 2000. 56: p. 983.
[9.] M.S. Morad and A.A.O. Sarhan, Application of some ferrocene derivatives in the field of corrosion inhibition. Corrosion Science, 2007. 50: p. 744.
[10.] P. Bommersbach, et al., Formation and behaviour study of an environment-friendly corrosion inhibitor by electrochemical methods. Electrochimica Acta 2005. 51 p. 1076.
[11.] S.M. Powell, H.N. McMurray, and D.A. Worsley, Use of the Scanning Reference Electrode Technique for the Evaluation of Environmentally Friendly, Nonchromate Corrosion Inhibitors. Corrosion, 1999. 55: p. 1040.
[12.] A.M. Alsabagh, M.A. Migahed, and Hayam S. Awad, Reactivity of polyester aliphatic amine surfactants as corrosion inhibitors for carbon steel in formation water (deep well water). Corrosion Science 2006. 48: p. 813.
[13.] M.A. Deyab, Effect of cationic surfactant and inorganic anions on the electrochemical behavior of carbon steel in formation water. Corrosion Science 2007. 49: p. 2315.
[14.] D. Choi, S. You, and J. Kim, Development of an environmentally safe corrosion, scale, and microorganism inhibitor for open recirculating cooling systems. Materials Science and Engineering 2002. A335: p. 228.
[15.] G. Moretti, F. Guidi, and G. Grion, Tryptamine as a green iron corrosion inhibitor in 0.5 M deaerated sulphuric acid. Corrosion Science 2004. 46: p. 387.
[16.] G. Shustak, A.J. Domb, and D. Mandler, Preparation and Characterization of n-Alkanoic Acid Self-Assembled Monolayers Adsorbed on 316L Stainless Steel. Langmuir 2004. 20: p. 7499.
[17.] I. Felhösi, E. Kálmán, and P. Póczik, Corrosion Protection by Self-Assembly. Russian Journal of Electrochemistry, 2002. 38: p. 230.
[18.] K. Aramaki and T. Shimura, Self-assembled monolayers of carboxylate ions on passivated iron for preventing passive film

breakdown. Corrosion Science, 2004. 46: p. 313.
[19.] S. Ramachandran, et al., Self-Assembled Monolayer Mechanism for Corrosion Inhibition of Iron by Imidazolines. Langmuir 1996. 12: p. 6419.
[20.] B. A. Boukamp, Equivalent Circuit Users Manuel; Report CT88/265/128, University of Twente, Department of Chemical Technology: The Netherlands. 1989.
[21.] J. Cruz, T. Pandiyan, and E. Garcia-Ochoa, A new inhibitor for mild carbon steel: Electrochemical and DFT studies Journal of Electroanalytical Chemistry, 2005. 583: p. 8.
[22.] H. Ashassi-Sorkhabi and N. Ghalebsaz-Jeddi, Inhibition effect of polyethylene glycol on the corrosion of carbon steel in sulphuric acid. Materials Chemistry and Physics 2005. 92: p. 480.
[23.] H. Ashassi-Sorkhabi and N. Ghalebsaz-Jeddi, Effect of ultrasonically induced cavitation on inhibition behavior of polyethylene glycol on carbon steel corrosion. Ultrasonics Sonochemistry, 2006. 13(2): p. 180.
[24.] S. Omanovic and S.G. Roscoe, Electrochemical Studies of the Adsorption Behaviour of Bovine Serum Albumin on Stainless Steel. Langmuir 1999. 15: p. 8315.
[25.] S. Modiano, C.S. Fugivara, and A.V. Benedetti, Effect of citrate ions on the electrochemical behaviour of low-carbon steel in borate buffer solutions. Corrosion Science, 2004. 46 p. 529.
[26.] H. Ashassi-Sorkhabi, et al., Corrosion inhibition of carbon steel in hydrochloric acid by some polyethylene glycols. Electrochimica Acta 2006. 51: p. 3848.
[27.] Qiu, L.G., et al., Synergistic effect between cationic gemini surfactant and chloride ion for the corrosion inhibition of steel in sulphuric acid. Corrosion Science, 2008. 50(2): p. 576-582.
[28.] S.A. Abd El-Maksoud and A.S. Fouda, Some pyridine derivatives as corrosion inhibitors for carbon steel in acidic medium. Materials Chemistry and Physics 2005. 93: p. 84.
[29.] S. Omanovic and S.G. Roscoe, Effect of Linoleate on Electrochemical Behaviour of Stainless Steel in Phosphate Buffer. Corrosion, 2000. 56: p. 684.
[30.] A. Yurt, et al., Investigation on some Schiff bases as HCl corrosion inhibitors for carbon steel. Materials Chemistry and Physics 2004. 85: p. 420.
[31.] C.H. Hamann and A. Hamnett, W. Vielstich in Electrochemistry, Wiley-VCH: Germany. 1998.
[32.] P. Saba, W.A.Brown, and S. Omanovic, Interactive Behaviour of Caffeine at a Platinum Electrode Surface. Mater.Chem.Phys, 2006. 100: p. 285.
[33.] R.K.R. Phillips, S. Omanovic, and S.G. Roscoe, Electrochemical Studies of the Effect of Temperature on the Adsorption of Yeast Alcohol Dehydrogenase at Pt. Langmuir, 2001. 17: p. 2471.
[34.] S. Omanovic and S. G. Roscoe, Interfacial Behaviour of beta-Lactoglobulin at a Stainless Steel Surface: An Electrochemical Impedance Spectroscopy Study. Journal of Colloid and Interface Science, 2000. 227: p. 452.
[35.] D. R. Jackson, S. Omanovic, and S. G. Roscoe, Electrochemical Studies of the Adsorption Behaviour of Serum Proteins on (cp)Ti. Langmuir 2000. 16 p. 5449.
[36.] A. Popova, et al., AC and DC study of the temperature effect on mild steel corrosion in acid media in the presence of benzimidazole derivatives. Corrosion Science 2003. 45: p. 33.
[37.] W. Furbeth, et al., Novel protective coatings based on a combination of self-assembled monolayers and conducting polymers Proceedings of EUROCORR, Nizza, France, 2004.